Spillover Reoxidation of Ceria Nanoparticles – Supporting Information

David C. Grinter[†‡], Chris Muryn[¶], Alessandro Sala[§], Chi-Ming Yim[†], Chi L. Pang[†], Tevfik O. Menteş[§], Andrea Locatelli[§] and Geoff Thornton[†]

[†]Department of Chemistry and London Centre for Nanotechnology, University College London, London, WC1H 0AJ, UK

[‡]Chemistry Department, Brookhaven National Laboratory, Upton, NY, 11973, USA

[¶]School of Chemistry and Photon Science Institute, University of Manchester, Manchester, M13 9PL, UK

[§]Elettra – Sincrotrone Trieste S.C.p.A, Basovizza, Trieste, 34149, Italy

Table of Contents

1. Estimation of ceria film thickness with XPS
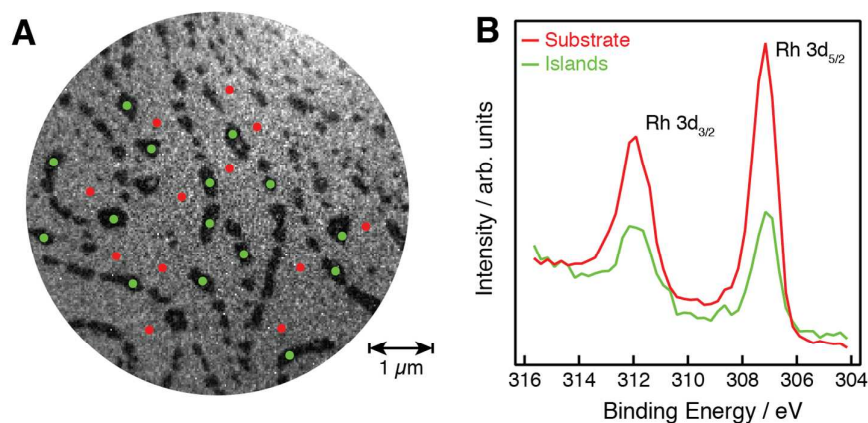
Figure S1. (A) Energy-filtered XPEEM image (hν = 450 eV) obtained at the maximum of the Rh $3d_{5/2}$ peak (B.E. = 307.2 eV); ceria islands appear as dark patches on a bright background due to their attenuation of the photoemission from the Rh(111) substrate. The areas from which the XPS spectra in B were obtained are highlighted in red and green. **(B)** Rh 3d XPS spectra (raw data) obtained from energy-filtered XPEEM of the bare substrate (red) and ceria islands (green).

In order to obtain an estimate of the ceria film thickness, energy-filtered XPEEM images were acquired over the Rh 3d region as displayed in Figure S1. From the image at the maximum of the Rh $3d_{5/2}$ peak (Figure S1A) it is possible to identify the locations of the ceria islands, which appear dark on a bright background. From the spectra (Figure S1B) obtained either on the bare substrate (red) or the islands (green), the attenuation due to the oxide islands can be measured. Using this attenuation and the calculated mean free path (0.9 nm) for the photoelectrons (K.E. = 140 eV) in CeO_2[1] it is possible to estimate the thickness as ~0.8 nm, i.e. 2-3 trilayers of ceria.

2. LEEM contrast after x-ray exposure
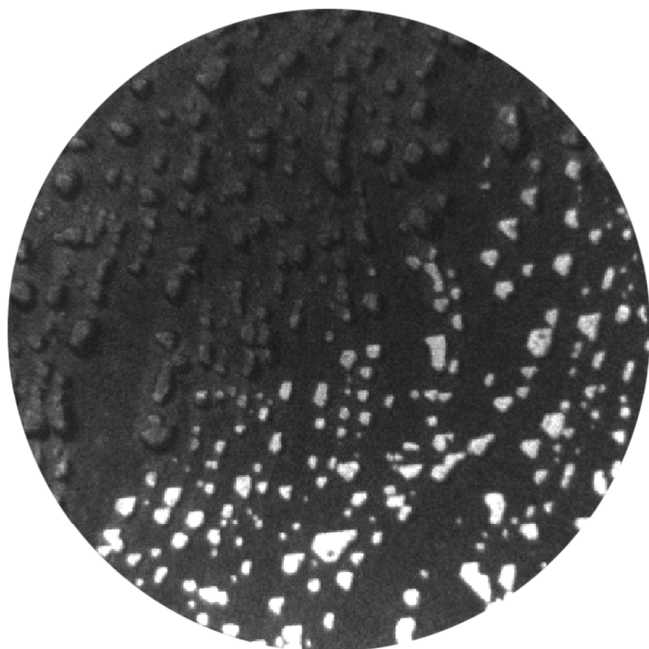
Figure S2. Large-area dark-field LEEM image (FOV = 6 μm, S.V. = 15 V) showing the result of prolonged (~ 30 minutes) illumination with soft X-rays (hν ~120 eV) on a 0.5 MLE CeO_2(111) film on Rh(111). Total photon exposure to the area at the top left of the frame was $\sim10^{20}$ ph.cm^{-2}

The contrast in the LEEM image in Figure S2 shows the effect of exposure to 120.8 eV soft X-rays for 30 minutes on our model CeO_2(111)/Rh(111) system (total exposure of $\sim10^{20}$ ph.cm^{-2}). The region in the top left was exposed to the beam, which comes in from the bottom left hand side and is elongated along that direction due to the grazing (16°) incidence on the sample. The more reflective ceria islands can be clearly observed in the non-exposed area in the bottom right.

3. Evolution of the ceria oxidation state during x-ray illumination under oxidising conditions
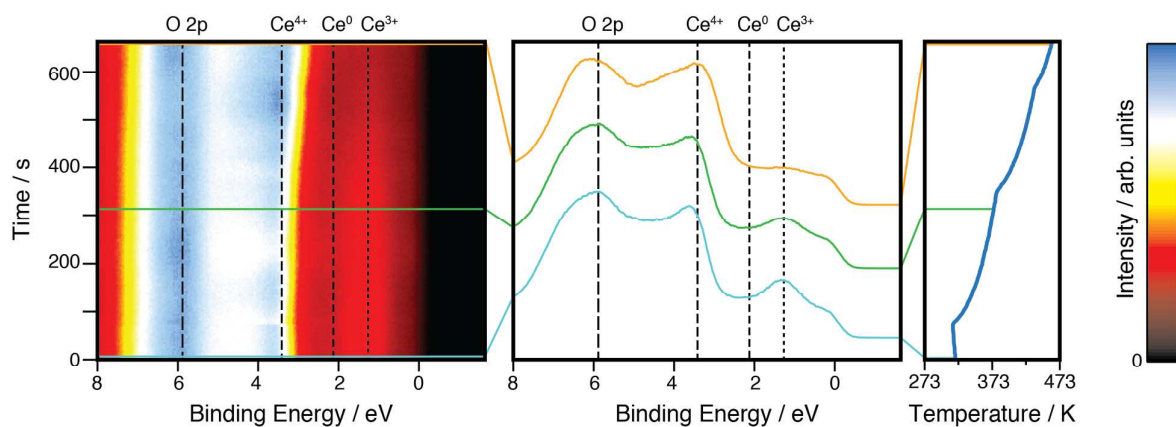
Figure S3. Resonant valence band XPS spectra of CeO$_x$(111)/Rh(111) under illumination with soft x-rays (hv = 120.8 eV) in 2×10^{-6} mbar O$_2$ as the temperature of the sample is ramped from 310 to 460 K.
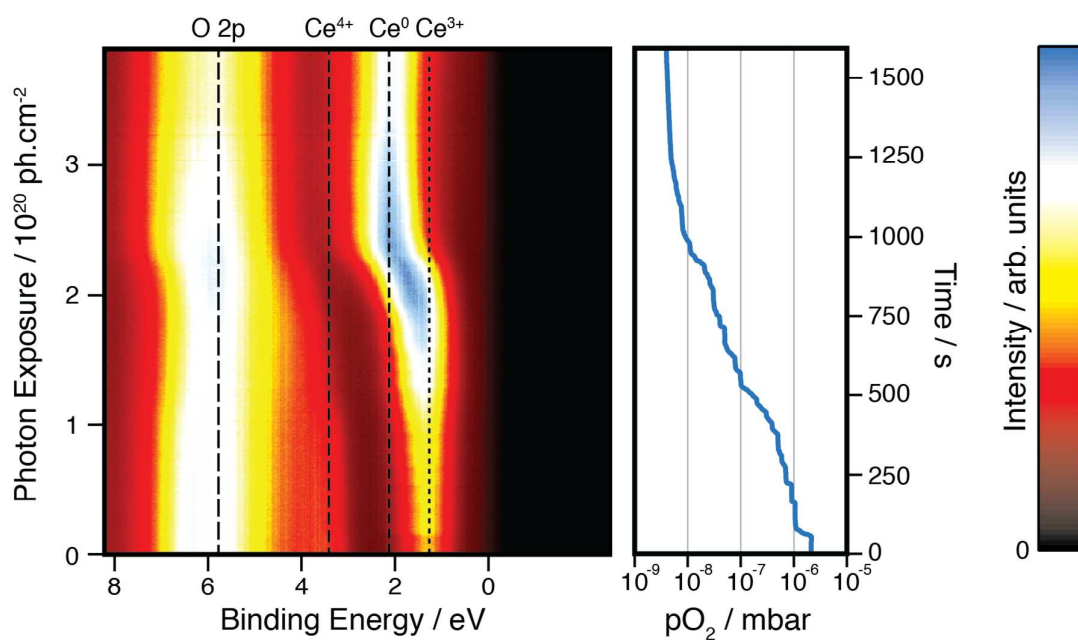
Figure S4. Resonant valence band XPS spectra of CeO$_x$(111)/Rh(111) under illumination with soft x-rays (hv = 120.8 eV) as the pO$_2$ within the chamber is decreased from 2×10^{-6} mbar to 5×10^{-9} mbar.

4. LEED evidence of reoxidation via O_2 exposure
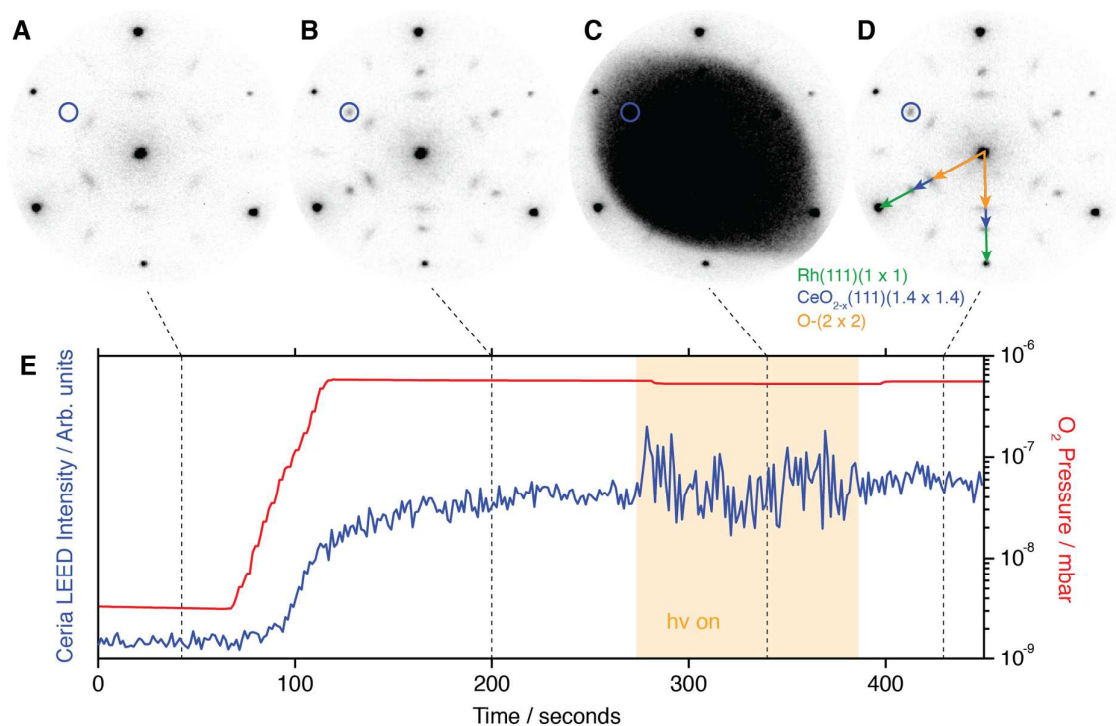
Figure S5. (A-D) LEED patterns (S.V. = 40 V) and **(E)** intensity plot as a 1 MLE $CeO_{2-x}(111)$ film on Rh(111) is reoxidized with O_2 at 300 K after prior X-ray–induced reduction of the surface. **(A)** LEED pattern of the damaged film ($pO_2 = 2.8 \times 10^{-9}$ mbar) with reflexes from Rh(111)(1×1) and O-(2×2) present. **(B)** LEED pattern of the reoxidized film ($pO_2 = 5 \times 10^{-7}$ mbar), the ceria spots at (1.4×1.4) relative to the substrate have been restored. **(C)** LEED pattern of the reoxidized film ($pO_2 = 4.6 \times 10^{-7}$ mbar) under irradiation with 120.8 eV X-rays. The high intensity in the center is due to the angle-resolved photoelectrons. **(D)** LEED pattern of the reoxidized film ($pO_2 = 5 \times 10^{-7}$ mbar) with the origins of the spots labelled: Rh(111)(1×1) substrate in green, $CeO_{2-x}(111)(1.4\times1.4)$ in blue, and O-(2×2) in orange. **(E)** Plot of the ceria LEED spot intensity (blue line, left axis) and O_2 pressure (red line, right axis) against time. The period of time when the sample was exposed to the X-rays is shaded.

The effect of reoxidizing by exposure to O_2 is also demonstrated by the changes observed in the LEED patterns of ceria films on Rh(111) as shown in Figure S5. A series of LEED patterns are displayed (A-D) above a plot (E) of the first-order ceria spot intensity (blue line, left axis) and O_2 pressure (red line, right axis) versus time (bottom axis). The initial LEED pattern (Figure S5A) is

obtained from a region of the film that was thoroughly irradiated (hv = 120.8 eV) for ~1 hr (total photon exposure: ~10^{21} ph.cm^{-2}). The intense Rh(111)(1×1) substrate spots as well as a diffuse O-(2 × 2) overlayer and extremely faint CeO$_{2-x}$(111)(1.4×1.4) are observed (compare to Figure 1A). O$_2$ is introduced into the chamber after ~65 seconds up to a maximum pressure of 5×10^{-7} mbar. When the O$_2$ pressure is above ~1×10^{-7} mbar the ceria spot intensity is seen to increase rapidly over a period of ~30 seconds and then plateau slowly. An image of the LEED pattern at the 200 second mark is displayed in Figure S5B. In addition to the substrate and overlayer spots in Figure S5A, there are now sharp, intense CeO$_{2-x}$(111) spots at (1.4×1.4) relative to the Rh(111)(1×1). To investigate whether X-rays play any role in the reoxidation process, at 275 seconds the valve to the beamline was opened and the sample illuminated with 120.8 eV soft x-rays for 110 seconds (a total photon exposure of 6×10^{18} photons.cm^{-2}) as depicted by the shaded area in Figure S5E. Although there is an increase in the noise due to the additional photoemission background (see pattern in Figure S5C) during the period of irradiation, the overall intensity of the ceria diffraction spots does not change, indicating that exposure to the photon beam in the oxygen partial pressure does not affect the oxidation or ordering of the ceria. The small drop in O$_2$ pressure (5×10^{-7} mbar to 4.6×10^{-7} mbar) during illumination with the beam is due to additional pumping occurring through the beamline. Figure S5D shows the pattern after 430 seconds (identical to that in Figure S5B) where the various reflexes are marked according to their origin; Rh(111)(1×1) substrate in green, CeO$_{2-x}$(111)(1.4×1.4) in blue, and O-(2×2) in yellow.

5. Temperature dependence of ceria/Rh(111) LEED pattern

A T = 350 K **B** T = 400 K

○ Rh(111) - (1 x 1)
○ CeO$_2$(111) - (1.4 x 1.4)
○ O - (2 x 2)
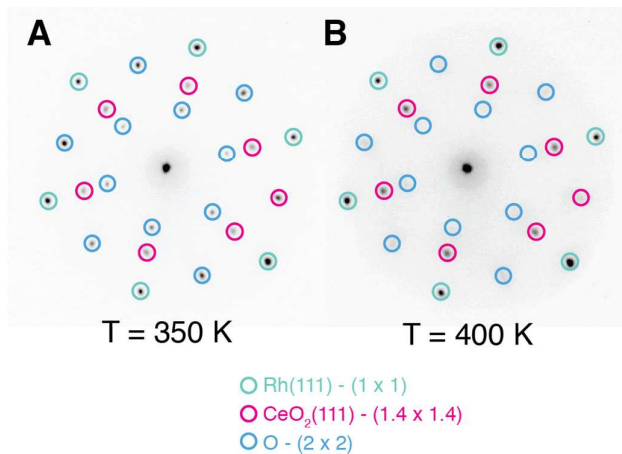
Figure S6. LEED patterns (S.V. = 40 V) of a 0.5 MLE CeO$_2$(111) film on Rh(111) at elevated temperatures: **(A)** 350 K, **(B)** 400 K in 5× 10^{-7} mbar O$_2$.

The LEED pattern of the ceria film on Rh(111) shows a strong temperature dependence, as shown in Figure S6 where measurements at (A) 350 K and (B) 400 K are compared. The spots for the CeO$_2$(111)-(1.4×1.4) (pink) and the Rh(111)-(1×1) (green) are intense and sharp at both temperatures, whereas those for the O-(2×2) (blue) are very weak and diffuse in Figure S6B, indicative of the high mobility of oxygen on the Rh surface at this higher temperature.

6. XPEEM/XPS analysis of carbon contamination
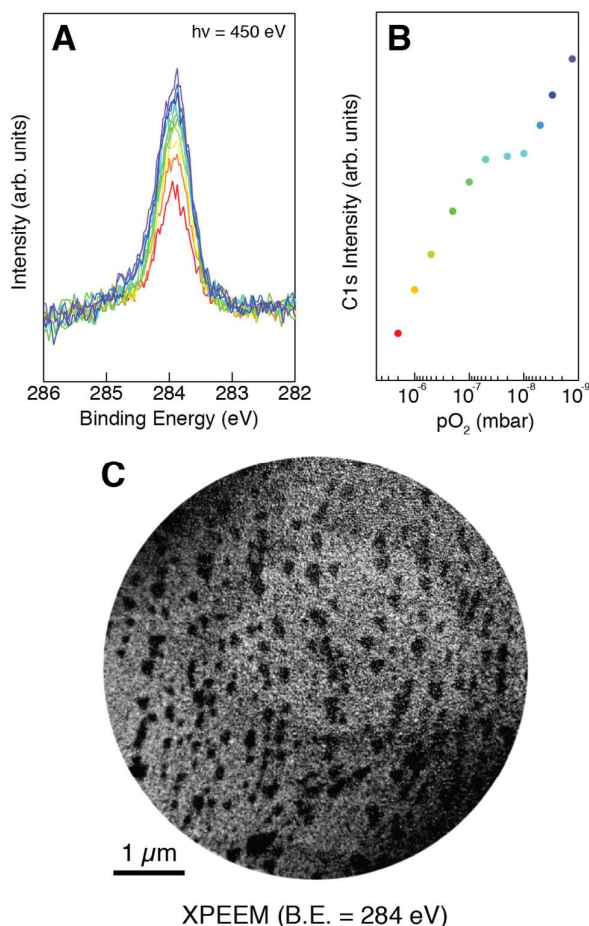
Figure S7. XPS and XPEEM imaging demonstrating carbon deposition onto the $CeO_x(111)/Rh(111)$ system under the x-ray beam. (**A**) C1s XPS (hν = 450 eV) acquired sequentially in the μ-XPS mode as the partial pressure of O_2 in the chamber was reduced from 2×10^{-6} mbar (red line) to 1.3×10^{-9} mbar (purple line) (**B**) Plot of the C1s intensity in (A) vs. O_2 pressure. (**C**) Energy-filtered XPEEM image obtained at the maximum of the C1s peak.

Carbon deposition under high flux x-ray illumination is commonly observed during synchrotron measurements, thought to be mainly a result of the cracking of CO and CO_2 present in the background vacuum.[2,3] In our experiments, we employ the dispersive plane XPS mode of the instrument to rapidly obtain high-resolution spectra of the C1s region and study any changes as the

partial pressure of O_2 within the measurement chamber is varied. C1s spectra are displayed in Figure S7A (intensities plotted in Figure S7B) as the pO_2 is decreased gradually from 2×10^{-6} mbar to 1.3×10^{-9} mbar. A clear increase in the carbon signal is observed as the oxygen is removed from the chamber, and in the intensity plot we can see an inflection point for the pressures in the range 1-3×10^{-8} mbar. Since the μ-XPS mode samples an area of the sample containing both ceria islands and the Rh substrate, we used energy-filtered XPEEM imaging detecting photoelectrons corresponding to the maximum of the C1s (B.E. = 284 eV) to examine exactly where the carbon deposition is occurring on the sample (Figure S7C). In this image the Rh substrate appears as bright and the ceria islands dark, thereby indicating that the majority of the carbon is deposited onto the metal rather than the ceria.

7. Resonant VB spectra of ceria reoxidation via oxygen spillover
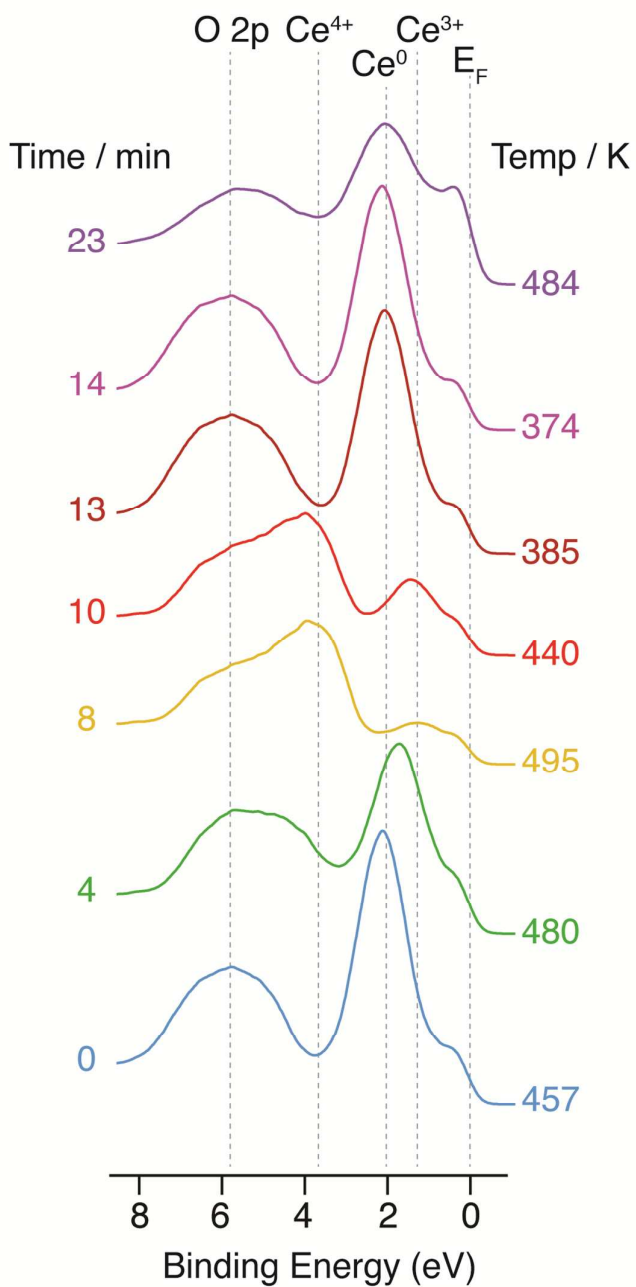
Figure S8. Resonant VB spectra of $CeO_{2-x}(111)/Rh(111)$ during cycles of heating/cooling in UHV to demonstrate the repeated re-oxidation of photon-reduced ceria by the O-(2 × 2) superstructure. Spectra are offset for clarity. $h\nu = 120.8$ eV.

To study the capacity of the O-(2 × 2) overlayer to reoxidize the ceria, the film presented in Figure 6C was once again cooled to 300 K and exposed to 120.8 eV soft x-rays. After this further reduction step, the temperature was again ramped (see Figure S8) to reoxidize. In this case it required heating to 495 K to fully re-oxidize (yellow spectrum in Figure S8). Presumably this increased temperature relative to the 475 K seen in Figure 6 demonstrates that oxygen from further than the immediate surroundings (which has likely been depleted by the previous annealing step) is required to "heal" the ceria. Upon cooling below 400 K, the ceria once again is reduced by the beam (red spectrum in Figure S8), however increasing the temperature again (purple spectrum in Figure S8) fails to reoxidize the ceria. At the end of this process the VB is composed of just a Ce^0 component and a much decreased O 2p region, which along with a very pronounced Fermi step indicates that the ceria is nearly completely reduced.
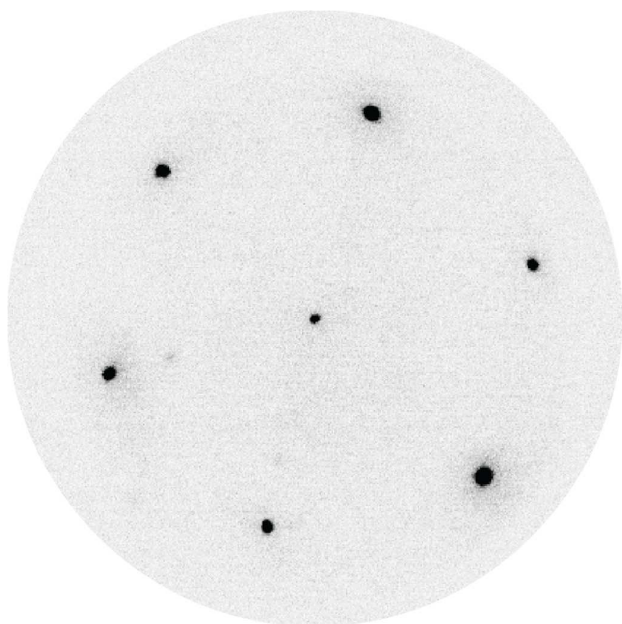
Figure S9. LEED pattern (40 eV) from the fully reduced ceria film after the process depicted in Figure S8. The CeO_2(111)-(1.4 x 1.4) is very faint and the O-(2 x 2) diffraction spots can no longer be seen.

After the process depicted in Figure S8, the ceria is fully reduced and the oxygen overlayer on the Rh(111) is depleted. This is further evidenced by the LEED pattern of the surface as shown in Figure S8, where strong Rh(111) spots are observed along with very faint ceria reflexes, and the oxygen spots are no longer present.

References

(1)   Tanuma, S.; Powell, C. J.; Penn, D. R. Calculations of Electron Inelastic Mean Free Paths (IMFPS). IV. Evaluation of Calculated IMFPs and of the Predictive IMFP Formula TPP-2 for Electron Energies Between 50 and 2000 eV. *Surf. Interface Anal.* **1993**, *20*, 77–89.

(2)   Günther, S.; Kolmakov, A.; Kovac, J.; Kiskinova, M. Artefact Formation in Scanning Photoelectron Emission Microscopy. *Ultramicroscopy* **1998**, *75*, 35–51.

(3)   Gregoratti, L.; Mentes, T. O.; Locatelli, A.; Kiskinova, M. Beam-Induced Effects in Soft X-Ray Photoelectron Emission Microscopy Experiments. *J. Electron Spectr. Relat. Phenom.* **2009**, *170*, 13–18.